ChemComm

Accepted Manuscript

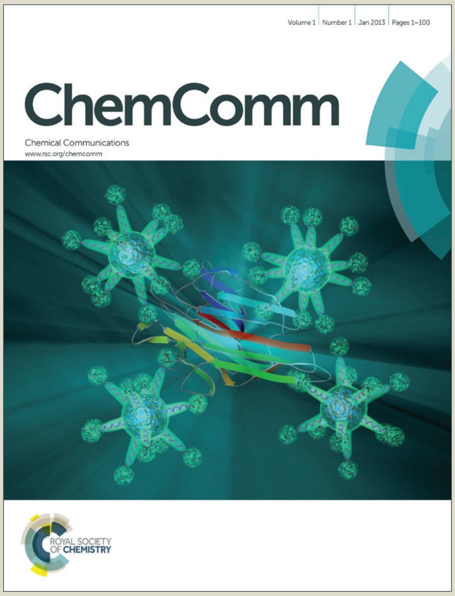

ROYAL SOCIETY OF CHEMISTRY

www.rsc.org/chemcomm

ChemComm RSCPublishing

COMMUNICATION

Cite this: DOI: 10.1039/x0xx00000x

On the chemistry of activating commercial carbon-supported PtRu electrocatalyst for methanol oxidation reaction

Received 00th January 2012,
Accepted 00th January 2012

DOI: 10.1039/x0xx00000x

www.rsc.org/

D.-J. Chen,[a,b] S.-G. Sun[b] and Y. Y. J. Tong[a]

Although potential cycling has been widely used to activate PtRu electrocatalysts for methanol oxidation, little is known about the molecular/atomic level chemistry involved so neither what constitutes the optimal activation. This important question is addressed herein by *in situ* attenuated total reflection–surface enhanced IR reflection absorption spectroscopy using methanol-generated CO as a probe.

For direct methanol (MeOH) fuel cells (DMFCs), PtRu is still among the best performing electrocatalysts for the anodic MeOH oxidation reaction (MOR)[1-4]. In fundamental studies of PtRu electrocatalysis for MOR, it is a common practice to subject the as-received PtRu to multiple potential cycling in the presence of MeOH until stable cyclic voltammetry is obtained, which serves as a catalyst activation process.[1, 5, 6] This is illustrated in Fig.1a where presented are the chronoamperometric (CA) measurements done at 0.495 V (all potentials reported here are referred to reversible hydrogen electrode (RHE) unless otherwise specified) on a commercial (Johnson-Matthey, or J-M) carbon-supported PtRu (1:1, 60 wt.%, and 3.1 nm average particle size) electrocatalyst (J-M PtRu/C) after subjecting it to a given number of potential cycles (Fig. S1, electronic supporting information, or ESI). As can be seen clearly from the inset, the initial potential cycles activate but further potential cycles deactivate the catalyst.

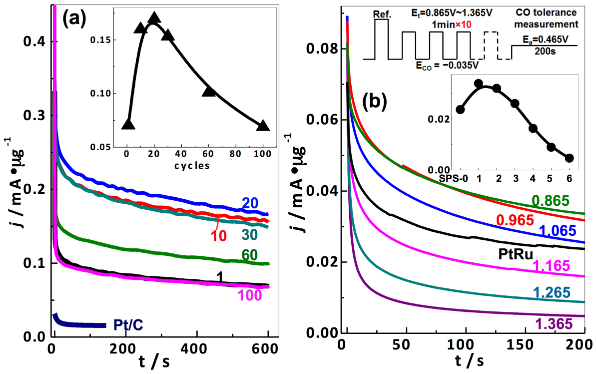

Fig. 1. CA curves of the J-M Pt/Ru/C deposited on GC (glassy carbon) after multiple potential cycles together with that of the J-M Pt/C as a reference (a) and the SPSs on Au film (b). The inset in (a) shows the potential-cycle-dependent mass specific MOR activity at 0.495 V. The insets in (b) are the schematic of an SPS and the SPS-dependent mass specific MOR activity at 0.465 V respectively.

However, little is known about the molecular/atomic level chemistry involved in such an activation-deactivation process: what does the activation process do to the surface of PtRu catalyst that leads to the substantial increase in MOR activity and what causes the deactivation? Such ill-defined knowledge leads to wide variations in the claims of having developed the best PtRu electrocatalysts in the literature, which in turn hinders better-focused development of superior electrocatalysts for MOR. In an attempt to address these both fundamentally and practically important questions, we designed a step-potential (SP) *in situ* ATR-SEIRAS protocol that used MeOH-generated, linearly bound CO (M-CO_L) as a molecular surface probe to follow the activation-deactivation process. The protocol, as schematically illustrated in the inset of Fig. 1b, was as follows. The as-received J-M PtRu/C catalyst was first drop-casted onto the pre-prepared Au film on a triangular silicon prism, air-dried completely, and assembled into an *in situ* IR cell (Fig. S2). The PtRu catalyst was then held at -0.035 V until current became negligible before being subjected to SP sequences (SPSs) of the

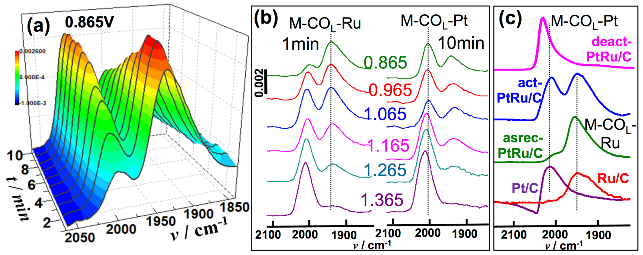

Fig. 2. In situ SEIRAS spectra of M-CO_L on the J-M PtRu/C: (a) the time-dependent IR spectra of CO during SPS-1; (b) the IR spectra of M-CO_L after the first (left) and tenth SP (right) as the SP value changes from 0.865 V to 1.365 V; (c) the IR spectra of M-CO_L on asrec- (green), act- (blue), deact- (magenta) PtRu, Pt/C (brown), and Ru/C (red), respectively.

in situ SEIRAS measurements in 0.1 M $HClO_4$ + 0.5 M MeOH. Each SPS consisted of a first 1-min SP at 1.065 V during which the reference IR spectrum was recorded and 10 sequential activation SPs at a constant given SP value that varied from 0.865 V to 1.365 V (SPS-1 to SPS-6, respectively) with an increment of 0.1 V by sequence. Any two consecutive activation SPs were separated by a 1-min base potential holding at -0.035 V during which IR spectra were recorded. Representative sequential spectra are shown in Fig. 2a for the SPS-1 (see Fig. S3 for the spectra of other SPSs). Fig. 2b compares the IR spectra recorded after the first activation SP (left) with that after the tenth activation SP (right) for the incremental activation SP values. After each SPS, the MOR activity was assessed by CA at 0.465 V for 200 s (notice that this potential is 30 mV smaller than the one used in Fig. 1a on a GC electrode in order to minimize any oxidation of MeOH-generated CO but still have decent MOR current). The measured CAs are presented in Fig. 1b, which reproduces what was observed in Fig. 1a, i.e., the same activation-deactivation process was observed. The corresponding normal and M-CO_L stripping CVs of the as-received, the best activated, and the worst deactivated PtRu/C samples in pristine 0.1 M $HClO_4$ electrolyte are shown in Figure S3.

Fig.2c compares the SEIRAS spectra of as-received (asrec-, before SPS-1), activated (act-, after SPS-2), and deactivated (deact-, after SPS-6) PtRu/C with those of commercial Pt/C and Ru/C. That two clearly distinguishable M-CO_L IR bands (~1952 cm^{-1} and ~2010 cm^{-1}), which can be reasonably assigned to CO_L on Ru-like (M-CO_L-Ru) and Pt-like (M-CO_L-Pt) sites respectively[7, 8], can be used to follow closely the chemistry of the activation-deactivation process. Fig. 3 shows the integrated IR band intensities of the M-CO_L-Pt (blue triangles), M-CO_L-Ru (red circles), and sum of the two (open squares) respectively as functions of time and the SP potential. Notice that all these IR measurements were carried out sequentially on the same starting sample and in the same IR cell after it being subjected to *accumulative* SPSs (inset in Fig.1b).

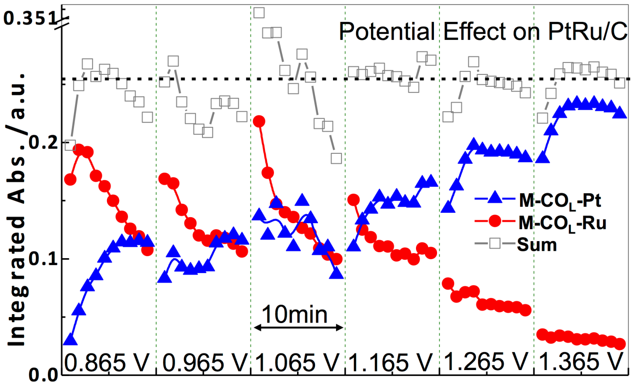

Fig, 3. The integrated IR band intensities of the M-CO_L-Pt (blue triangles), -Ru (red circles), and sum of the both (open squares) as a function of time per a given SPS and of the SPS.

While the sum of the amounts of M-CO_L-Pt and -Ru remained relatively constant over the entire 60-minute measurements, as indicated by the horizontal dashed line, the individual amounts of the M-CO_L-Pt and -Ru varied substantially (Fig. 2a/2b and Fig. S3), indicating the very dynamic nature of the catalyst surface composition during the activation/deactivation. For SPS-1 and -2, the catalyst surface started with a surface dominated by the M-CO_L-Ru[9] but ended with almost equal amounts of the M-CO_L-Pt and –Ru. The catalyst showed highest MOR activity after SPS-1 and -2. That the amount of M-CO_L-Ru at the beginning of SPS-3 was approximately the same as those of SPS-1 and -2 suggests that there was no significant loss (if any) of surface Ru. However, the MOR activity started dropping after SPS-3, coinciding with a decrease in the amount of M-CO_L-Ru as indicated by its substantially decreased integrated IR intensity at the beginning of SPS-4. The latter trend persisted for SPS-5 and -6, indicating a continuous loss of Ru that was highly likely responsible for the deactivation of the catalyst. The corresponding SEIRAS spectrum recording at the 10th min of the SPS-6 (Fig.2b) indicates that there was almost no surface Ru left after the SPS-6.

The above observations were supported further by the TEM (transmission electron microscope) and EDS (energy dispersive X-ray spectroscopy) measurements as presented in Fig. 4. As can be seen, the act-PtRu/C had a size of 2.9±0.7 nm, almost the same as the asrec-PtRu/C (3.1±0.7 nm). But the deact-PtRu/C saw a clear size increase to 3.8±0.7 nm, indicating a sintering effect of over-activation. Moreover, there was also no elemental composition change for the act-PtRu/C, as measured by EDS that gave Pt:Ru = 51:49 for the sample. This is practically the same as 50:50 of the asrec-PtRu/C considering the uncertainties in the measurements. In great contrast, the deact-PtRu/C had Pt:Ru = 67:33, confirming the substantial lost of Ru in the deact-PtRu/C. This is corroborated by the more and more Pt-like CV as shown in Fig. S3. Considering that the dispersion of a 3-nm particle is ~40%, the loss of ~ 50% of Ru is consistent with the full depletion of surface Ru for the deact-PtRu as indicated by the IR spectra of the SPS-6 shown in Fig.2b. The insets in Fig. 4(a) to 4(c) are high-resolution TEM images of the respective PtRu/C NPs. The white straight lines highlight the atomic planes. That the same inter-atomic-plane distance was observed in all three samples indicates that the core of the PtRu NPs were still in an alloyed form.

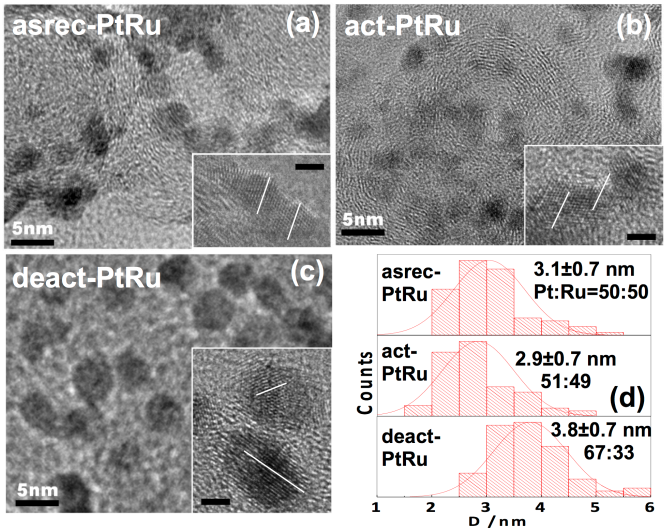

Fig. 4. The TEM images of the asrec-PtRu (a), act-PtRu (b), and (c) deact-PtRu. (d) shows the size distributions of the three samples (200 counts per sample) and their elemental ratios measured by EDS. The insets in (a) through (c) are high resolution TEM images with the white straight lines highlighting the atomic planes and crystallinity of the samples. The scale bars are 5 nm and 2 nm for the main images and the insets respectively.

That these two IR bands of the act-PtRu/C had their peak positions overlap exactly with those of M-CO$_L$ on the respective carbon-supported pure Ru and Pt nanoparticles (NPs), Fig.2c, suggests strongly that those Ru-like and Pt-like sites on the act-PtRu/C were segregated to form island-like structures. The blue shift of the dominant M-CO$_L$-Ru band and the red shift of the minor M-CO$_L$-Pt shoulder on the asrec-PtRu/C as compared to the CO$_L$ peak positions on their respective mono-metal samples are consistent with its alloyed nature. This is supported by XRD (X-ray diffraction) measurements on the asrec-, act-, and deact-PtRu/C respectively, as presented in Fig. 5. Using the peak position at ~40.5° (Fig. 5a), lattice constant and alloy degree (Vegard's Law) of the samples can be calculated[10]. The act-PtRu/C had a larger lattice constant of 3.8915Å as compared to that of the asrec-PtRu/C (3.8638 Å). The former also had a lower alloying degree (0.19) than that of the latter (0.42). Notice that the lattice constant calculated for the asrec-PtRu/C is very close to but slightly larger than that (3.8626 Å) of a polycrystalline PtRu alloy with Pt:Ru = 48.3:51.7 reported in the literature[1], which gives the confidence to our calculations. Since no Ru was lost for the act-PtRu/C, lower alloying degree is consistent with the proposed Ru segregation on the surface. Moreover, the act-PtRu/C also showed a broad but discernable diffraction peak at 58.3° (indicated by the left vertical dashed line in Fig. 5b) that overlaps with that of Ru(102) (PDF2: 00-002-1258) as shown by the XRD pattern of the Ru/C (black) in Fig. 5b. This again indicates the presence of segregated Ru in the act-PtRu. However, that the PtRu (220) peak at ~67° was still clearly observable in act- and deact-PtRu/C, as indicated by the right vertical dashed line in Fig.5b, suggests that there was still significant amount of alloyed phase in these two samples, presumably inside the NPs, which is consistent with the HRTEM images (insets in Fig. 4).

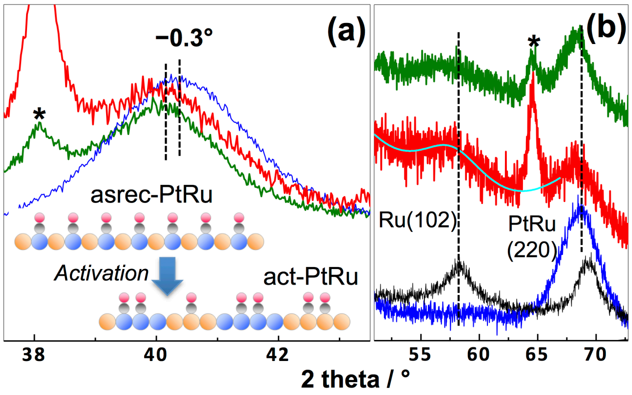

Fig. 5. The XRD patterns of the asrec-PtRu (blue), act-PtRu (red), and deact-PtRu (green). The black spectrum in (b) was from Ru/C, shown here as a reference. The stars indicate the peaks from the underlying Au thin film deposited on the Si prism for SEIRAS. The schematic inset in (a) illustrates the proposed activation process. Orange, blue, black and pink balls stand for the Pt, Ru, C and O atoms respectively.

Conclusions

In summary, our *in situ* ATR-SEIRAS investigation of the activation-deactivation process taking place in a commercial J-M PtRu/C electrocatalyst, which was corroborated by TEM, EDS, and XRD measurements, revealed that the commonly used catalyst activation procedure caused dynamic re-distribution of surface Pt and Ru that moved the catalyst surface from the initial alloyed distribution of Pt and Ru to more segregated distributions of each element, as illustrated by the inset in Fig.5a. The best activation corresponded to achieving an equal amount of segregated surface Pt and Ru ensembles, presumably to maximize the Pt-Ru boundaries. However, over-activation led to deactivation of the catalyst, largely caused by the substantial loss of surface Ru. Notice that just simply holding the PtRu electrocatalyst at a reductive potential cannot activate the catalyst properly, i.e., no significant MOR activity gain can be obtained (result not shown here). This is probably because a simple potential holding cannot induce elemental redistribution on the surface. Thus, multiple potential cycling still is *the* procedure of catalyst activation. However, in order to prevent over-activation, the up-limit potential should not go beyond 0.965 V. On the other hand, it is unclear why the dissociative adsorption of MeOH on the alloyed surface led to a dominance of the M-CO$_L$-Ru. We speculate that it might have to do with that Ru is not a good element for dehydrogenation but Pt is. So the dissociative adsorption of MeOH on alloyed surface would start with binding the carbon atom to Ru then followed by sequential dehydrogenation on the neighbouring Pt, which led to CO on Ru which apparently did not diffuse to the neighbouring Pt sites. But the other way around would not work.

Acknowledgements: This work was supported by a grant from DOE-BES (DE-FG02-07ER15895) to YYJT. DJC was an exchange PhD student from SGS's lab where the research is supported by the NSFC (21229301, 21321062). The authors thank Mr. Yangwei Liu from the Tong Lab for taking the TEM images and the UMD NISP Lab for use of its TEM facility. The EDS results were obtained at the Georgetown GNuLab.

Notes and references

[a] Department of Chemistry, Georgetown University, 37th & O Streets, NW, Washington, DC 20057. Email: yyt@georgetown.edu.

[b] [2]Departments of Chemistry and State Key Laboratory for Physical Chemistry of Solid Surfaces, Xiamen University, Xiamen 361005 P R China. Email: sgsun@xmu.edu.cn.

Electronic Supplementary Information (ESI) available: [details of any supplementary information available should be included here]. See DOI: 10.1039/c000000x/

1. H. A. Gasteiger, N. Markovic, P. N. Ross and E. J. Cairns, *The Journal of Physical Chemistry*, 1993, **97**, 12020-12029.
2. T. Iwasita, *Electrochimica Acta*, 2002, **47**, 3663-3674.
3. O. A. Petrii, *Journal of Solid State Electrochemistry*, 2008, **12**, 609-642.
4. M. Watanabe and S. Motoo, *Journal of Electroanalytical Chemistry*, 1975, **60**, 267-273.
5. Q. Lu, B. Yang, L. Zhuang and J. Lu, *The Journal of Physical Chemistry B*, 2005, **109**, 1715-1722.
6. H. Wang, L. R. Alden, F. J. DiSalvo and H. c. D. Abruña, *Langmuir*, 2009, **25**, 7725-7735.
7. W. F. Lin, M. S. Zei, M. Eiswirth, G. Ertl, T. Iwasita and W. Vielstich, *The Journal of Physical Chemistry B*, 1999, **103**, 6968-6977.
8. T. Yajima, H. Uchida and M. Watanabe, *The Journal of Physical Chemistry B*, 2004, **108**, 2654-2659.
9. C. J. Pelliccione, E. V. Timofeeva, J. P. Katsoudas and C. U. Segre, *The Journal of Physical Chemistry C*, 2013, **117**, 18904-18912.
10. E. Antolini and F. Cardellini, *Journal of Alloys and Compounds*, 2001, **315**, 118-122.